

Fig. 4 Pressure distributions computed on inlet centerbody. Symbols represent present solution; broken lines represent solution of Ref. 3.

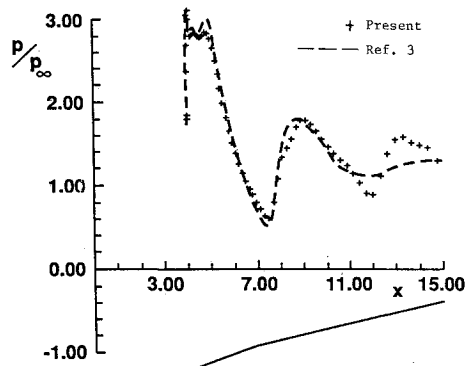


Fig. 5 Pressure distributions computed on cowl inner surface. Symbols represent present solution; broken lines represent solution of Ref. 3.

here, the incorporation of multigrid enables convergence to the steady state in the equivalent of 125 iterations for the four-grid level calculation.

References

- ¹Caughey, D. A., "A Diagonal Implicit Multigrid Algorithm for the Euler Equations," *AIAA Journal*, Vol. 26, July 1988, pp. 841-851.
- ²Jameson, A., Schmidt, W., and Turkel, E., "Numerical Solution of the Euler Equations by Finite-Volume Methods Using Runge-Kutta Time-Stepping Schemes," *AIAA Paper 81-1259*, June 1981.
- ³Chaussee, D. S. and Pulliam, T. H., "Two-Dimensional Inlet Simulation Using a Diagonal Implicit Algorithm," *AIAA Journal*, Vol. 19, Feb. 1981, pp. 153-159.
- ⁴Jameson, A., "Multigrid Solution of the Euler Equations," *Mechanical and Aerospace Engineering*, Princeton Univ., Princeton, NJ, MAE Rept. 1316, June 1983.
- ⁵Caughey, D. A. and Jameson, A., "Accelerated Iterative Calculation of Transonic Nacelle Flow Fields," *AIAA Journal*, Vol. 15, Oct. 1977, pp. 1474-1480.

Görtler Instability of Wall Jets

J. M. Floryan*

University of Western Ontario,
London, Ontario, Canada

Introduction

It has recently been shown by Floryan¹ that Görtler instability might occur over concave as well as convex walls, provided that the velocity distribution inside the boundary layer

violates the inviscid stability criterion.¹ It has also been suggested¹ that when velocity distribution is nonmonotonic, the flow will consist of layers that alternatively violate and satisfy the stability criterion, and this could lead to an interesting evolution of the unstable motion. The purpose of this Note is to analyze the stability of a simplest flow of this type, i.e., a wall jet over a concave surface, which consists of an inviscidly unstable layer located next to the wall and an inviscidly stable layer located farther away. The appropriate velocity field is described by Glauert.² The required disturbance equations and the method of solution are described in Ref. 3. The same problem has been considered by Kahawita;⁴ however, the present analysis, which is much more extensive, is based on a model rationally incorporating the effects of boundary-layer growth³ and, therefore, the present results represent a considerable improvement over the results of Ref. 4.

Results

The disturbance growth process⁵ is illustrated in Figs. 1-6. Figure 1 displays curves of constant spatial amplification rate β as a function of the spanwise wave number α and the Görtler number $G = U_\infty \delta_r / \nu (\delta_r / R)^{1/2}$ (where R denotes the radius of curvature of the wall). The wall-jet thickness, $\delta_r = (\nu \Phi / U_\infty)^{1/2}$, is the length scale, where U_∞ is the maximum of the streamwise velocity component of the jet, ν the kinematic viscosity, and Φ the distance from the virtual origin of the jet. The neutral curve corresponds to $\beta = 0$, and its minimum occurs for $\alpha \rightarrow 0$; the critical value of the Görtler number is $G_c \approx 1.0$. Because there is no critical wave number, the wavelength selection mechanism is determined by the disturbance growth process. It is convenient to introduce a dimensionless wavelength parameter $\Lambda = F^{1/3} \lambda^{1/3} \nu^{-1} (\lambda / R)^{1/3}$ (which is constant in the flow direction) in order to follow streamwise development of a vortex of a constant dimensional wavelength λ (dimensionless wave number α changes in the flow direction because of variations of the length scale δ_r). Here F is the dimensional "flux of external momentum flux."² Straight lines with slope 5/6 correspond to constant Λ in Fig. 1. One might presume that the vortex described by Λ that stays closest to the line of maximum amplification in Fig. 1 has the most favorable conditions to grow. Figure 2 displays the total amplification of disturbances that occurred between the neutral curve and streamwise locations

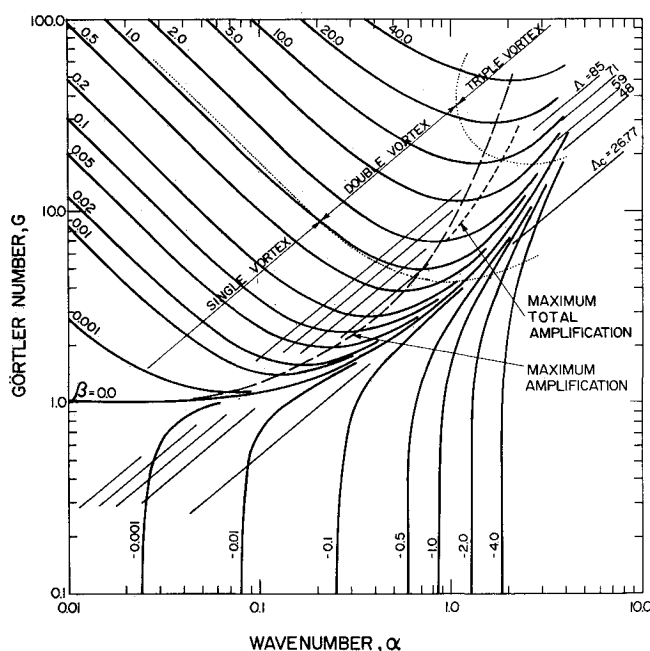


Fig. 1 Curves of constant amplification rate β as a function of Görtler number G and wave number α for the first mode of the Görtler instability of wall jets over a concave wall.

corresponding to Görtler numbers of $G = 5.0, 10.0, 15.0$, and 20.0 . The total amplification is defined as³

$$A = \exp \int_{G_0}^G \frac{4}{3} \frac{\beta}{G} dG$$

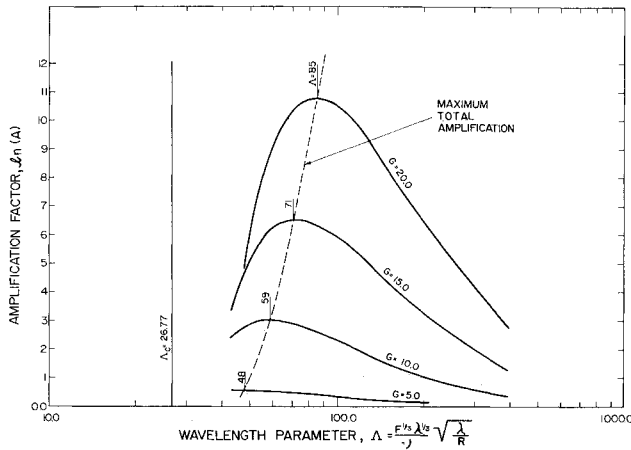


Fig. 2 Curves of the total amplification of the first-mode disturbances as a function of the wavelength parameter Δ at the streamwise locations, corresponding to Görtler numbers of $G = 5.0, 10.0, 15.0$, and 20.0 .

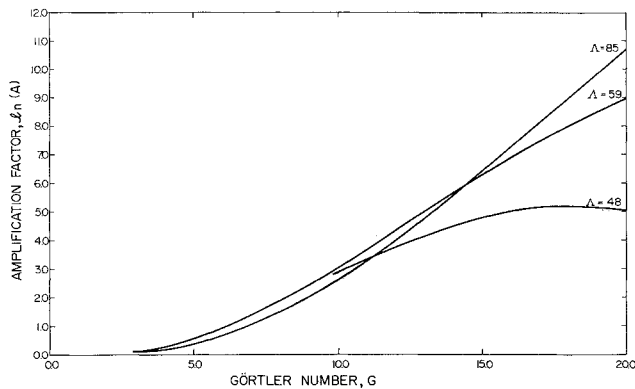


Fig. 3 Curves of the total amplification of the first-mode disturbances as a function of Görtler number G .

where $A(G_0) = 1$. Here A denotes the amplitude of the disturbances, and subscript 0 stands for the initial conditions. Each integration begins at the neutral curve and follows the same vortex defined by the constant dimensional wavelength λ . The results show that the maximum total amplification shifts from $\Delta = 48$ at $G = 5.0$ to $\Delta = 85$ at $G = 20.0$. This is in contrast to the Blasius boundary layer, where the maximum total amplification occurred within the same range of Δ , regardless of the streamwise location.⁵ It is known from experimental observations of boundary layers that the wavelength selection mechanism acts only up to the establishment of vortices, which are then preserved downstream, regardless of the local growth rates.⁵ This points out the importance of the very initial stages of the instability process and suggests that one should expect the vortices of $\Delta = 48.0$ to dominate. The cutoff wavelength parameter defining the lower bound of the unstable wavelengths is $\Delta_c = 26.77$ and is considerably smaller than in the case of the Blasius boundary layer.⁵

The disturbance growth process is illustrated in Fig. 3. All vortices grow initially in a similar manner. When the Görtler number becomes sufficiently large, the rate of growth of smaller vortices gradually decreases and then becomes negative, suggesting the existence of a self-stabilization mechanism. The variations of disturbance velocity field as a function of the Görtler number and corresponding to $\Delta = 71$ are displayed in Fig. 4 (the curve corresponding to $\Delta = 71$ almost overlaps with $\Delta = 85$ in Fig. 3). The eigenfunctions have been scaled by imposing condition $\max(u) = 1$. At the neutral curve, the velocity field has a form of one layer of vortices. Further downstream, at Görtler number slightly larger than 5.0 , the velocity field splits into two layers of vortices and, at $G \approx 17.00$, the upper vortex splits into two, resulting in three layers of vortices. The streamwise location of the vortex split can be correlated with the form of the disturbance velocity field. The streamwise disturbance velocity component has a form very similar to the mean flow at the neutral curve (Fig. 4). Further downstream the vortex becomes compressed closer to the wall. When the center of the vortex reaches the location of the maximum of the mean flow velocity, the vortex split occurs. The second split occurs when the first vortex is further compressed so that its center reaches a location halfway between the location of the maximum of the mean flow velocity and the wall. These additional vortices have very small amplitude and could not be well represented in Fig. 4. The qualitative form of the vortex split phenomenon is similar for other values of Δ and conditions under which it occurs are shown in Fig. 1. Only the first vortex

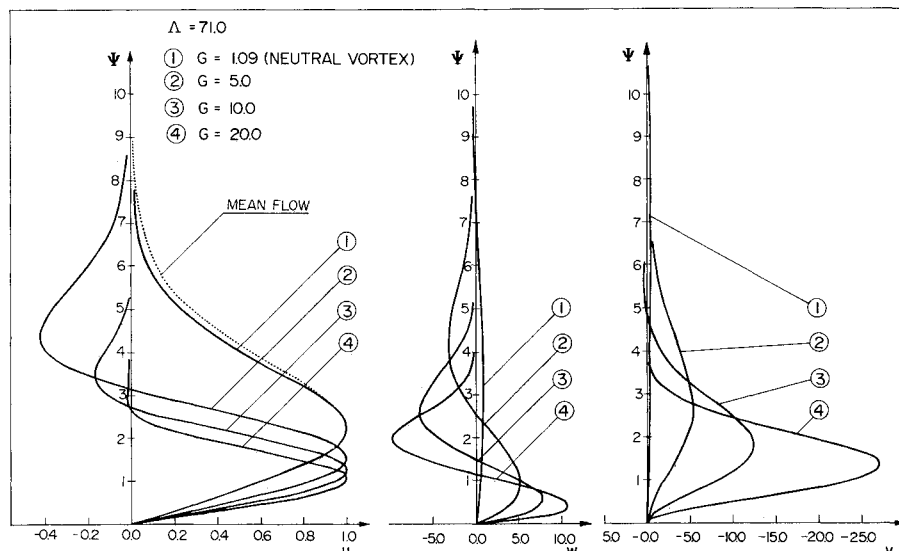


Fig. 4 Disturbance velocity fields for the disturbances associated with the wavelength parameter $\Delta = 71$ at the downstream locations corresponding to $G = 1.09, 5.0, 10.0$, and 20.0 . Here u, w, v stand for the streamwise, spanwise, and normal-to-the-wall velocity components, respectively, and Ψ denotes coordinate in the direction normal to the wall.

Fig. 5 Neutral curves for the first and second modes of the Görtler instability of wall jets.

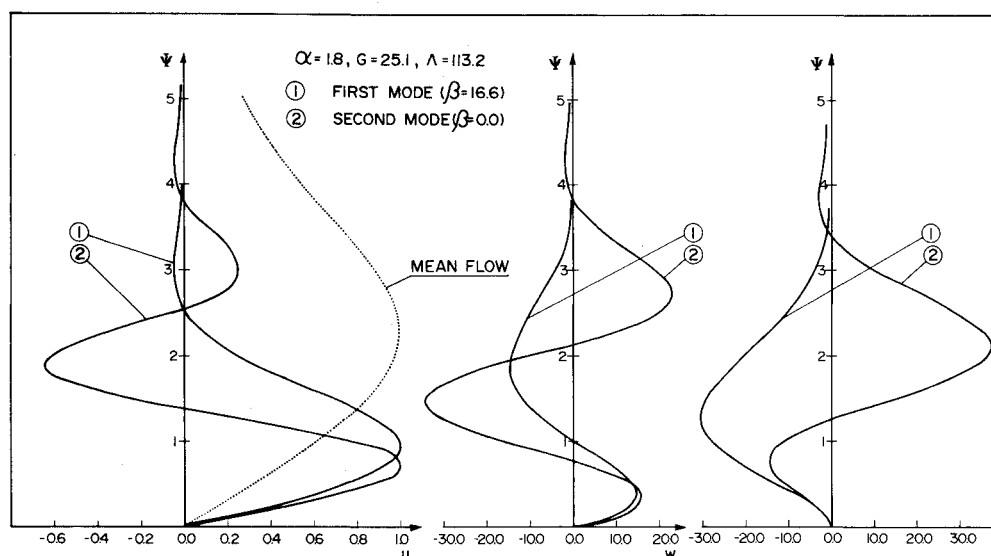
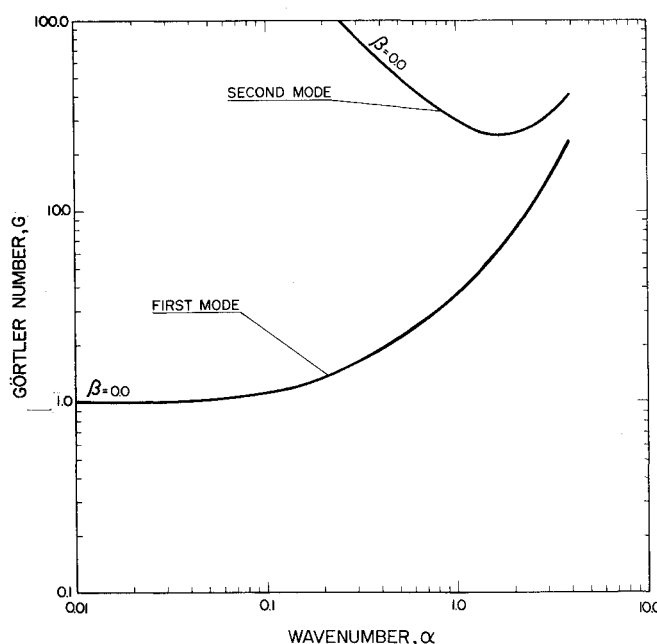


Fig. 6 Disturbance velocity fields for the first and second modes of the Görtler instability of wall jets.

is driven directly by the instability forces because it contains the part of the jet that is inviscidly unstable. The additional vortices are driven by shear stresses acting between different layers of vortices and, through an increased dissipation, they tend to weaken the instability motion. This is well illustrated in Fig. 1, where the neutral curve begins to bend to the left close to the location of the first vortex split, thus increasing the range of stable Λ . If the instability was dominated by the vortices $\Lambda = 48$, the jet would eventually stabilize itself (Figs. 1 and 3). The idea of self-stabilization could be utilized in stabilizing boundary layers through tangential blowing.

The existence of several layers of vortices raises a question as to whether they were correctly identified as the first instability modes. The neutral curves corresponding to the first and second modes are given in Fig. 5. The first and second mode eigenfunctions under the same flow conditions are plotted in Fig. 6. The results show that the basic concept, in which it is assumed that the first mode consists of one layer of vortices, the second of two layers, etc., needs re-evaluation.

Conclusions

Görtler instability of wall jet over a concave surface has been analyzed. The results suggest that the fundamental instability

mode may have a form of one, two, and more layers of vortices, depending on the flow conditions. The unstable motion is expected to originate in the form of a single layer of vortices, which separates subsequently into two, three, or more distinct layers further downstream. The increased dissipation resulting from the vortex split phenomenon could lead to a self-stabilization of vortices of short wavelengths.

Acknowledgments

This work was supported by a grant from the Natural Sciences and Engineering Research Council of Canada.

References

- ¹Floryan, J. M., "Görtler Instability of Boundary Layers Over Concave and Convex Walls," *Physics of Fluids*, Vol. 29, Aug. 1986, pp. 2380-2387.
- ²Glauert, M. B., "The Wall Jet," *Journal of Fluid Mechanics*, Pt. 6, Vol. 1, Dec. 1956, pp. 625-643.
- ³Floryan, J. M. and Saric, W. S., "Stability of Görtler Vortices in Boundary Layers," *AIAA Journal*, Vol. 20, March 1983, pp. 316-324.
- ⁴Kahawita, R. A., "Instability of Laminar Wall Jets Along Curved Surfaces," *AIAA Journal*, Vol. 13, Nov. 1975, pp. 1517-1518.
- ⁵Floryan, J. M. and Saric, W. S., "Wavelength Selection and Growth of Görtler Vortices," *AIAA Journal*, Vol. 22, Nov. 1984, pp. 1529-1538.